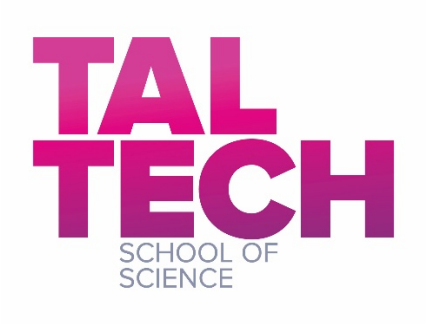

Design and implementation of a system for single myofibril force measurements

Bachelor thesis

Student: Maike Mona Širinov
Supervisors: Marko Vendelin, Professor
Martin Laasmaa, Professor
Laboratory of Systems Biology
Study program: Applied Physics

Tallinn 2023

Üksiku müofibrilli jõu mõõtmise süsteemi disain ja rakendus

Bakalaureusetöö

Üliõpilane: Maike Mona Širinov
Juhendajad: Marko Vendelin, professor
Martin Laasmaa, professor
Süsteemibioloogia labor
Õppekava: Rakendusfüüsika

Tallinn 2023

Declaration

Hereby I declare that I have compiled the paper independently and all works, important standpoints and data by other authors have been properly referenced and the same paper has not been previously been presented for grading.

Author: Maike Mona Širinov
[Signature, date]

The paper conforms to requirements in force.
Supervisors:

Marko Vendelin
[Signature, date]

Martin Laasmaa
[Signature, date]

Permitted to the defence.
Chairman of the Defence Committee: [Name]
[Signature, date]

Contents

Abstract

For gaining comprehensive understanding of the mechanics of heart muscle contraction, it is essential to perform measurements at the subcellular level. Single myofibril preparations are highly suitable for this purpose as they are devoid of other cellular systems and possess a small diameter, ensuring minimal diffusion-related delays.

The aim of this work was to set up a system that allows single myofibril force measurements. This type of setup is required in the laboratory to study regulation of contraction and its properties.

The first part of this thesis gives an general overview of existing methodologies related to instrumentation for measuring force from single myofibrils, methods for isolating myofibrils, and the mechanics of myofibrils. The subsequent section of this thesis outlines the methods employed in this study and presents the corresponding results.

The setup for measuring force from myofibrils was constructed. It comprises microneedles made from glass capillaries that were affixed to the ends of myofibrils and function as force sensors, exhibiting deflection during contractions.

This system will be further developed to facilitate precise measurement of force across various calcium concentrations.

Annotatsioon

Selleks, et täielikult mõista südamelihase kontraktsiooni mehaanikat, on oluline läbi viia mõõtmiseid subtsellulaarsel tasemel. Üksikute müofibrillide preparaadid on selle jaoks väga sobivad, kuna neil puuduvad muud rakusüsteemid ja neil on väike diameeter, mis tagab minimaalse difusioonist tuleneva viivituse.

Selle töö eesmärk oli luua süsteem, mis võimaldab mõõta jõudu üksikult müofibrillilt. Seda tüüpi seade on laboris vajalik, et uurida kontraheerumise regulatsiooni ja selle omadusi.

Lõputöö esimene osa annab üldise ülevaate olemasolevatest metoodikatest, kirjeldades jõu mõõtmise aparatuuri, müofibrillide isoleerimise tehnikaid ja müofibrillide mehaanikat. Selle lõputöö järgmises osas kirjeldatakse selles töös kasutatud meetodeid ja esitatakse saadud tulemused.

Töötati välja süsteem üksikute müofibrillide jõu mõõtmiseks, mis koosneb klaaskapillaaridest valmistatud mikronõeltest, mis toimisid kui jõuandurid. Nõelad kinnitati müofibrillide otstele. Kaltsiumi lisamisel lahusesse müofibrillid kontraheerusid, mille tulemusena kinnitatud nõelad paindusid, võimaldamaks mõõta jõudu.

Seda süsteemi arendatakse edasi, et järgnevalt mõõta jõudu müofibrillidelt erinevate kaltsiumi kontsentratsioonide juures.

Abbreviations

ADP	adenosine diphosphate
AFM	atomic force microscopy
ATP	adenosine triphosphate
ATPase	adenosine triphosphatase
BDM	2,3-butanedione-monoxime
Ca-SPOC	calcium spontaneous oscillatory contractions
CCD	charge-coupled device
MAVA	mavacamten
PFE	passive force enhancement
poly-HEMA	polyhydroxyethylmethacrylate
RFE	residual force enhancement

Introduction

The cardiac muscle is the muscle that makes up the walls of the heart. It is an important muscle as it is responsible for supplying oxygen and nutrients throughout the body by continuously pumping blood. It works involuntarily, meaning it contracts and relaxes without conscious control. Any abnormal contractility can indicate heart failure which is a global concern affecting millions of people [1, 2, 3]. Therefore, studying the heart muscle is essential to improving our understanding of heart function and ideally developing treatments and preventive measures for heart failure.

The 20th century saw great advancements in the field of muscle research as many important discoveries were made. With the help of new technologies, scientists were able to delve deeper into the workings of muscle tissue and gain new insights into how muscles contract and function. The discovery of the sliding filament theory in the 1950s by A.F. Huxley, H. Huxley and their contributors [4, 5] was a major breakthrough in understanding the mechanism of muscle contraction and has remained the accepted theory to this day. Despite the discoveries, much remains unknown, and thus, further research is required.

Many different measurements on muscle fibers and cells have been made so far but not as many on smaller elements. For detailed understanding of muscle structure, measurements on subcellular level are necessary, starting from myofibrils to single filaments. Myofibrils are striated muscle organelles composed of aligned sarcomeres which are the smallest contractile units of a muscle consisting of thin and thick filaments. Measuring force from a single myofibril can provide information that is not disturbed by other cellular systems, allowing control of the environment surrounding the contractile element. By changing the physiological environment, changes in muscle function can be assessed. For instance, how force in myofibrils responds to different levels of calcium, which plays an important role in the excitation-contraction coupling system. Since the measured elements are many times smaller, there is also reduced delay imposed by diffusion. The problem in single myofibril measurements is the difficulty of handling these small samples. Attaching the contractile element to the measuring device is a great hurdle.

The aim of this thesis is to set up a system that allows single myofibril force measurements for studying regulation of contraction and its properties in line with the other studies in the laboratory. In order to accomplish that, it is necessary to explore previously published setups. While taking into account the future objectives, the setup will be designed by utilizing the available hardware.

1 Theoretical basis

1.1 Cardiac muscle structure and function

Cardiac muscle, also known as myocardium, is a striated muscle that makes up the walls of the heart. The muscle fibers have a unique branching pattern (Figure 1) and are composed of interconnected cardiac muscle cells called cardiomyocytes [6, 7]. The cells contain numerous myofibrils, which are made up of aligned sarcomeres. Sarcomeres are the basic contractile units of muscle and consist of thick and thin filaments that slide past each other during contraction. Thin filaments are composed of actin, tropomyosin and troponin complex. The actin filaments form the backbone of the thin filament, while the tropomyosin wrap around the actin filaments. The troponin molecules are interspersed between the tropomyosin and actin. Thick filaments are composed of the protein myosin, which has a long tail and a globular head. The filaments give the muscle a striated appearance which is visible under a microscope as alternating light and dark bands.

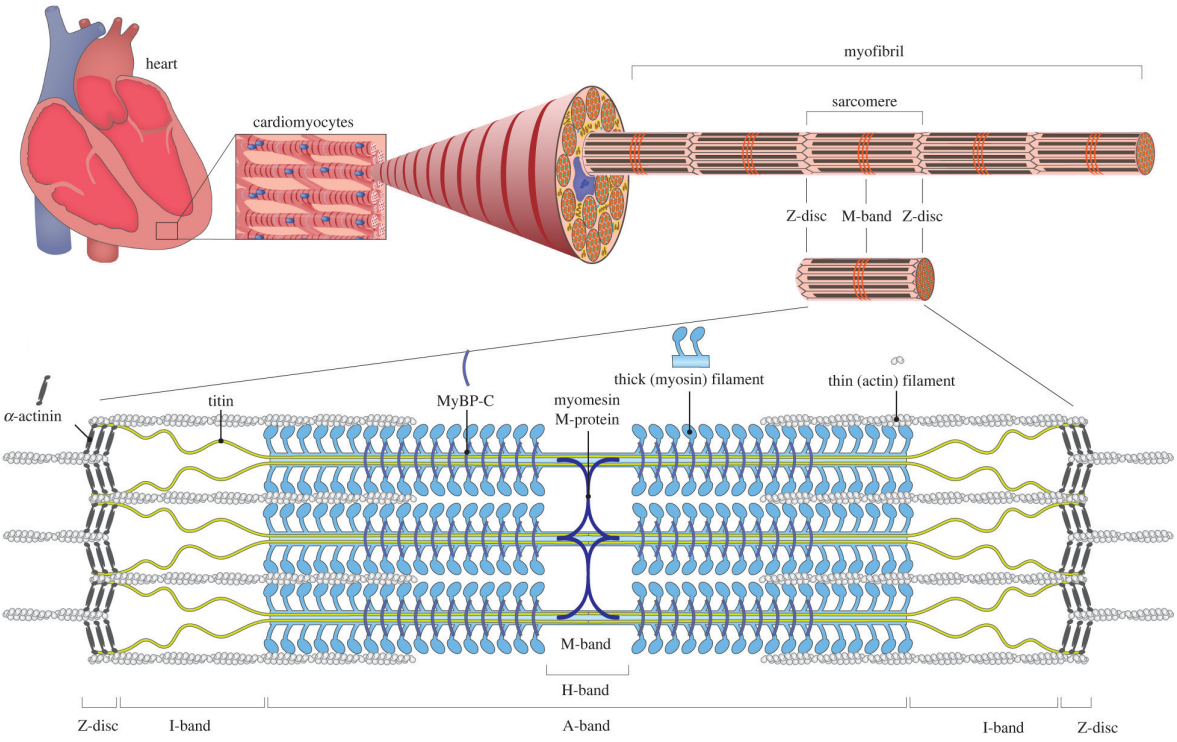

Figure 1. Hierarchical scheme of the cardiac structure and simplified illustration of a sarcomere. CC BY 4.0. Ahmed et al. Adapted from [7].

The sarcomere, seen in Figure 1, is bordered by Z-lines that also act as an anchoring point for actin filaments. The A band, which contains thick and thin filaments, appears darker when observed with a transmission light microscope, and is located at the center of the sarcomere. The I band, which contains the thin filaments, appears lighter and is located on either side of the A band. The H zone, located within the A band, contains only thick filaments and appears lighter than the rest of the A band. The M line is located at the center of the H zone, to which

myosin filaments are attached on opposite sides [7]. Titin is a giant protein that provides structural support and elasticity, located from the Z-disc to the M-line [6]. Alpha actinin is a protein that attaches actin filaments to the Z-disc [8].

During muscle contraction, the energy required is generated by the hydrolysis of adenosine triphosphate (ATP) molecules. The process of muscle cell contraction involves a series of steps known as the crossbridge cycle. In the initial released state, the myosin binding site on actin is blocked by tropomyosin and no interaction occurs between the filaments. The myosin head is in a low-energy position with ATP bound to it. ATP is hydrolyzed to adenosine diphosphate (ADP) and phosphate, causing the myosin head to move to a high-energy position while the myosin binding site on the actin filament remains blocked. Activation of the cell leads to the influx of calcium ions, which bind to troponin and cause tropomyosin to be displaced from the myosin binding site, allowing the myosin head to bind to the actin filament and form a crossbridge. Release of the phosphate bound to the myosin head causes the myosin head to undergo a power stroke, which results in movement along the actin filament, leading to muscle contraction. Finally, the release of ADP allows for the binding of a new ATP molecule, resulting in the release of the myosin head. If the calcium concentration remains high, the crossbridge cycle continues [9].

1.2 Setup for myofibrillar measurements

Multiple approaches exist for studying myofibril mechanics. The following review will examine previously published methodologies.

Commonly used setup for myofibril force measurements is built around an inverted microscope, as in [10]. The key elements of the apparatus are shown in Figure 2. The experimental system includes micromanipulators for manipulating and positioning myofibrils. The myofibrils are attached to two microneedles, one of which functions as a force transducer, while the other is linked to a piezo motor to induce length changes in the myofibril. The force transducer is connected to a data acquisition system, which records the force output from the myofibril as it contracts. A perfusion system is used to deliver different solutions to the myofibril. The system also includes a temperature control unit that maintains a constant temperature to ensure precise and consistent measurements. The chamber temperature is controlled by using a solution circulating through the channel surrounding the experimental bath. The experiments have been carried out at varying temperatures, ranging from 10°C [11, 12, 13], 15 °C [14, 15, 16] and 17 °C [10], as well as at room temperature (20-24°C) [17, 18, 19, 20]. The complete setup is positioned on an antivibration table [10].

In the experiments, a droplet of myofibrillar suspension is placed in the chamber filled with relaxing solution and left for 5-10 min to allow the myofibrils to sink to the bottom [21]. Single myofibril or bundles with good striation pattern are fixed at their ends to microneedles which are controlled by micrmanipulators. The experiments are done few micrometers above the chamber surface. The myofibril state is switched from relaxation to contraction by changing the solution in the bath chamber from a low calcium concentration solution to a high calcium concentration solution. The solution level in the bath chamber is maintained at a constant

level using a peristaltic pump [10].

For studying fast dynamic processes, rapid solution changes are induced by a piezo actuator that moves the double-barreled pipette, with outer diameter around 0.1 mm, within 10 ms to expose the myofibril to one stream or the other stream. Distance between the pipette tip and the myofibril is 0.4 - 0.6 mm [22].

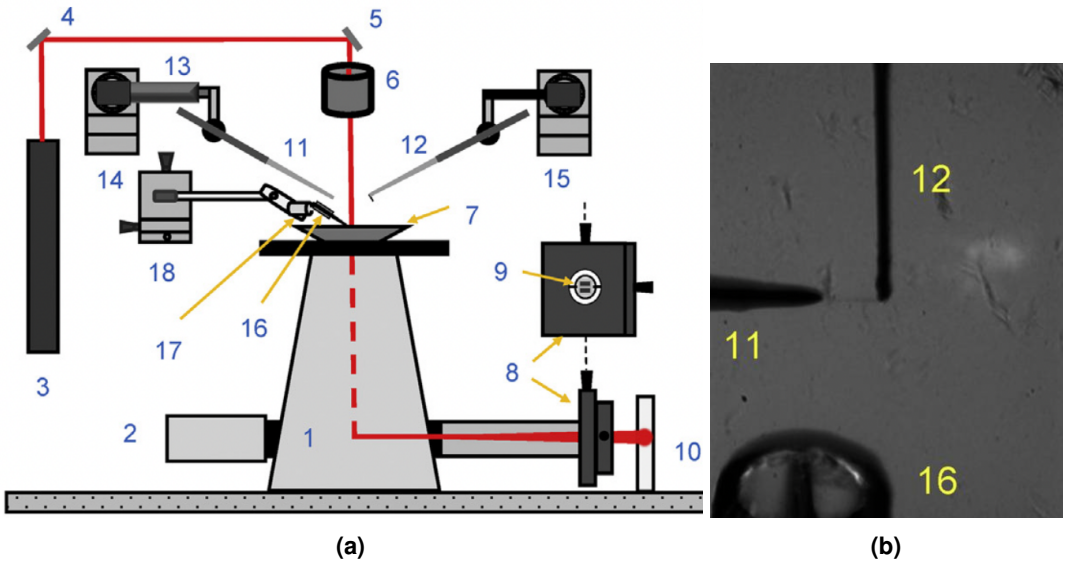

Figure 2. Setup for myofibril force measurements. (a) Experimental setup showing the key elements of the apparatus. (b) Two microneedles holding a small myofibril bundle. The numbers on the figures indicate: 1 - inverted microscope; 2 - camera; 3 - laser; 4 and 5 - mirrors; 6 - microscope condenser; 7 - bath mounted onto a microscope stage; 8 - XY positioning stage; 9 - segmented photodiode; 10 - projection plane for visual control of cantilever positioning; 11 - left microneedle; 12 - right microneedle (cantilever force sensor); 13 - piezo actuator; 14 and 15 - left and right micromanipulators for the positioning of left and right microneedle, respectively; 16 - double-barreled pipette; 17 - stepper motor controlling the position of the double-barreled pipette; 18 - XYZ positioning stage for the ultrafast two solutions switching system. CC BY 4.0. Vikhorev et al. Adapted from [10].

When measuring force from myofibril, it is also important to measure the sarcomere length as the generated force depends on the initial sarcomere length [23]. This can be done by analysing light intensity signal obtained from myofibril with the use of a linear photodiode, where sarcomere length is the distance between contiguous A-band intensity peaks. Phase contrast illumination is employed to enhance contrast between the darker A-bands and lighter I-bands [16, 18, 24, 11]. The centroids of the peaks are detected by a minimum average risk algorithm [25]. Occasionally, it is possible to visualize the Z-lines and sarcomere length can be confirmed based on the distance between adjacent Z-lines [26].

1.2.1 Microneedle production and calibration

The microneedles, to which the myofibrils are attached, are made from capillary glass tubing [10, 16, 27, 28]. The glass is pulled using a vertical pipette puller and the tip is bent by heating with microforge so that it is more or less aligned parallel to the plane of the specimen.

Prior to force measurements, it is essential to calibrate the microneedles, as the stiffness of the microneedle is required to calculate force. One way of doing that is by a cross-bending

method [16] which uses a pair of microfabricated cantilevers of known stiffness as reference beams [29]. The stiffness can be altered by adjusting cantilever length and width. The pulled glass microneedles are pressed orthogonal to their lengths against the microfabricated cantilevers, and the displacements can be measured. The microneedle stiffness K_n is calculated according to the formula:

$$K_n = \frac{K_c d_c}{d_n}, \tag{1}$$

where K_c is stiffness of the cantilever, d_c displacement of the cantilever and d_n displacement of the microneedle [16].

Some laboratories use atomic force microscopy (AFM) cantilever (Figure 3) as a force probe. The cantilever stiffness K is determined by measuring its dimensions through scanning electron microscope images as in [30] and calculated using

$$K = \frac{3EI}{L^3}, \tag{2}$$

where E is the Young's modulus, I is the moment of inertia of the cantilever cross section, and L is the length of the cantilever from the base to the point where force is applied.

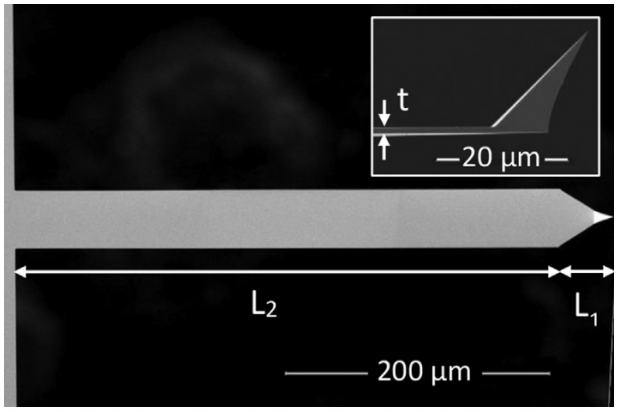

Figure 3. Scanning electron microscope image of AFM cantilever. The cantilever profile changes from rectangular to triangular at the tip of the cantilever. The inset is a side view of the cantilever.

The moment of inertia of a rectangular cross section is given by

$$I = \frac{WT^3}{12}, \tag{3}$$

where W is the width of the cantilever, and T is thickness of the cantilever.

The cantilever has a rectangular profile at its base with length L_2, and a triangular profile at its tip with length L_1. Both of the profiles have the same rectangular cross section with different widths, but the same thickness, T. The change in width is approximated by the average cantilever width $\overline{W}$, which is given by

$$\overline{W} = \frac{L_2}{L} W + \frac{L_1}{L} \frac{W}{2}, \tag{4}$$

where the $\frac{W}{2}$ term approximates the average width during the triangular part of the cantilever profile and the terms $\frac{L_2}{L}$ and $\frac{L_1}{L}$ represent the ratio of the length from the rectangular profile and the triangular profile, respectively. For simplicity, the cantilever stiffness can be rewritten as

$$K = \frac{3E}{L^3}\left[\frac{1}{12}\left(\frac{L_2}{L}W + \frac{L_1}{L}\frac{W}{2}\right)T^3\right] \tag{5}$$

[30].

The force sensing cantilever stiffness can vary between experiments. The stiffnesses used in myofibril experiments range from 30 to 1000 nN/µm [11, 14, 17, 31, 32]. While the force sensing cantilever is deflectable, the microneedle for myofibril length changes is relatively stiff. The ratio of the deflectable to the inflexible needle stiffness typically ranges from 0.02 to 0.1 [11, 12, 33].

1.2.2 Microneedle attachment

For attaching the microneedles at the ends of the myofibril, the tips of the needles are usually precoated with glue. The most commonly used glue is a watercuring silicone adhesive 3145 RTV, Dow Corning [11, 18, 20, 26, 34]. Another commonly used is 3140 RTV, Dow Corning, which has slightly lower viscosity [35]. The two adhesives, 3140 and 3145 RTV, are also used as a mixture of them both [29, 36] or with 2% nitrocellulose in amylacetate [13]. In addition, shellac and 70% ethanol mixture can also be used as glue [21].

Secure attachment should be confirmed, beacause the myofibril may pull free from the glue on subsequent activations [20, 33]. Glue integrity can be verified by monitoring the number of sarcomeres in the myofibril before and after activation. More sarcomeres between the glued needle tips after a protocol suggests that slippage of the myofibril in the glue has occurred [21]. To ensure firm attachment, the myofibril can be wrapped several times around each tip before the glue cures. This increases the contact area between the myofibril and the glue, improving the strength of the attachment [18].

While glue provides a reliable method for firm attachment, there has also been laboratories that optionally do not use glue and instead rely on the property of the myofibril to adhere to glass [33, 37, 38]. They use myofibrils that are floating in the chamber [33, 37] or myofibrils that have only one end attached to the glass surface [38].

The procedure of attachment without the use of glue is as follows [38]: firstly, one microneedle (L) is placed beneath the floating end of the myofibril and slightly drawn up, having the end of the myofibril loosely attached to needle. The other microneedle (R) touches the other end of the myofibril from above. Then, the needle L is carefully, without slackening nor overstretching, moved over needle R. The same procedure is repeated once more for the other needle by moving needle R over needle L. As a result the myofibril is wrapped around the microneedles.

The force applied by a single sarcomere is equivalent to that of a single myofibril and is calculated using

$$F(t) = \frac{Kd(t)}{N_m}, \tag{6}$$

where $F(t)$ is the force per myofibril as a function of time t, N_m is the number of myofibrils in a tested bundle, $d(t)$ is the displacement of the cantilever tip, and K is the stiffness of the force sensing cantilever [11].

1.2.3 Force measurements

When a myofibril is activated or stretched, it generates force that pulls on the force sensing cantilever. The force signal is obtained by detecting changes in the reflected laser beam from the cantilever using a photodiode [12, 13, 14, 39]. In case of a split photodiode as in [10], the laser beam is directed onto the cantilever and the image of the cantilever tip is projected between the two light sensitive areas of the double photodiode. The laser beam illuminates the photodiode cells and generates a current that is proportional to the intensity of the light illuminating the corresponding photodiode cell. The current output of the photodiodes is dependent on the displacement of the cantilever. The current difference between the two photodiodes is proportional to the deflection of the force probe.

An alternative method for detecting microneedle displacements is by image processing [38]. The positions of the microneedles are detected by setting a threshold for brightness in two windows around the needles. In the windows, black-and-white pictures are superimposed on a phase contrast image. The positioning is also indicated by the use of pixels on the monitor after averaging the position of the edge for each needle. This method is more suitable for measuring static properties, such as resting tension, rather than fast dynamic properties.

The force normalized to a cross sectional area is described as tension. The determination of the cross sectional area of the myofibril is uncertain due to technical constraints that allow for the measurement of the myofibril width in only one plane. To calculate the cross sectional area, it is assumed that the width and depth of the myofibril are equal and the form is circular [21].

1.3 Preparation of myofibrils

The dissected tissue is first placed in a 50:50 rigor/glycerol solution with protease inhibitors and stored in a freezer at -20°C for one week to a month to permeabilize the cellular membranes [12, 19, 24, 26, 36]. Rigor solution is used to preserve the structural integrity of the myofibrils. It typically contains a high concentration of salts, such as potassium chloride or sodium chloride.

The glycerinated tissue is minced and futher skinned in rigor solution containg 0.5% or 1% (v/v) Triton X-100 at 4°C for an hour or two [34, 19]. The use of Triton X-100 for skinning results in the removal of all membranous structures, leaving behind only intact myofilaments [40]. It is important to use the lowest effective concentration of Triton X-100 to reduce the risk of damaging the contractile proteins [11].

After skinning, the solution is changed to a new one without Triton X-100 and the sample is homogenized with a blender, leaving a suspension containing individual myofibrils. The homogenization is performed at various rates and durations [11, 12, 16, 34]. Homogenized

myofibrils are stored at 4°C and used for up to 5 days [14]. The homogenate may be filtered through 22 µm polypropylene meshes to remove aggregates of overcontracted myofibrils and large bundles [22].

The tissue stored in glycerol can also be homogenized first and then, just before the force measurements, skinned with 0.1% (v/v) Triton X-100 for 10 min in the experimental chamber [17, 33].

Another option is to permeabilize fresh or frozen at -80°C tissue using only 1% Triton X-100 for 3-4 hours [22, 41].

A novel method is obtaining myofibrils from primary cardiomyocyte culture [15]. Myocytes are obtained by enzymatic digestion and maintained in serum free condition which decreases the rate of dedifferentiation, with 5 days as the upper limit for maintaining myocytes in culture. After enzymatic digestion, the myocytes are collected in a cold relaxing solution containing either 20% sucrose to impose an osmotic shock or 0.01% Triton X-100 to cause complete lysis of cardiomyocytes. The sucrose method yields better quality of myofibrils. The mechanical properties of myofibrils obtained from a myocyte culture system are equivalent to those prepared by skinning tissue with Triton X-100.

One benefit of obtaining myofibrils from a primary culture system is the ability to manipulate specific cellular processes, enabling to investigate the effects of various interventions on the myofibrils. The cells can be treated with inhibitors or ectopically expressed proteins. Wherease generating transgenic or knockout animal is more time consuming and incurring a higher cost [15].

1.4 Mechanics of myofibrils

Myofibril-based mechanical studies offer several advantages over studies performed on isolated muscle fibers for evaluating sarcomeric protein function. With isolated muscle fibres, thousands of sarcomeres are arranged parallel in series and measured simultaneously. Length measurements on these fibers are typically based on average estimates, which may not accurately represent the behavior of individual sarcomeres. Also, the ultrastructural damage of myofibrils in fibers can contribute to impaired contractility, which can make it difficult to accurately measure the force of fiber contractions. In contrast, if structural damage is present in single myofibrils, they likely break during isolation or during the experiment [21]. Moreover, due to the small diameter and the lack of other cellular systems, diffusion of small molecules into myofibrils is completed within 2 ms, making them a non-diffusional limited model to study force kinetics [42, 43].

Acitive tension refers to the force generated in responce to a stimulus, which is typically induced in myofibril preparations by exposing them to an activation solution with a high concentration of calcium. Ca^{2+} concentration in experimental solutions is expressed as pCa, which is defined as

$$pCa = -log[Ca^{2+}]. \tag{7}$$

The force-pCa relationship is fitted by non-linear regression to the Hill equation:

$$F = \frac{F_0}{1 + 10^{-n(pCa_{50} - pCa)}} \tag{8}$$

where F_0 is the maximal active force at pCa 4.5, n is the Hill coefficient and pCa_{50} is the [Ca^{2+}] at the half maximal active force [17].

Sudden increase in Ca^{2+} concentration induces a single exponential force development with a rate constant k_{act} which is indistinguishable from k_{redev} , the rate constant of isometric force redevelopment following a period of unloaded shortening during steady-state activation [22]. Maximum isometric force is usually reached at pCa 5.0-4.5 with the maximum active isometric tension in the single rabbit cardiac myofibril at sarcomere lengths of 2.1-2.3 µm bieng 145 $\pm$ 35 mN/mm^2 [19].

The force-generating properties are influenced by Ca^{2+} concentration and the lattice spacing, which refers to the distance between the thick and thin filaments within a sarcomere. This spacing changes as the sarcomere lengthens or shortens, and affects the amount of overlap between the filaments [17]. The length-dependent activation is one of the mechanisms that contribute to the Frank-Starling law, which describes the increase in contractility with increased filling of the heart [44].

Multiple compounds could be added to the perfused solution to measure its effect on the force produced by the myofibril. For instance, addition of 1 mM 2,3-butanedione-monoxime (BDM), a myosin adenosine triphosphatase (ATPase) inhibitor, to activating soltuion causes a decrease in isometric force [26]. Additionally, the impact of medication on contractile proteins could be evaluated. For an example, mavacamten (MAVA), an inhibitor of myosins used for hypertrophic cardiomyopathy treatment, reduces maximal Ca^{2+}-activated isometric force, which is explained by the decrease in the number of heads functionally available for interaction with actin [14]. MAVA works by reducing the contractility of the myocardium through decreasing the affinity between actin and myosin filaments, and restoring a more balanced ratio of myosin heads in the relaxed conformation [45]. MAVA also has a strong inhibitory effect on Ca^{2+} -independent ADP-stimulated contractions, where relaxing solution (pCa 9.0) is used with reduced MgATP and higher MgADP concentration [14].

Isolated myofibril preparations offer a unique opportunity to observe the intricate features of contractile units in exquisite detail. As force is measured, several observable characteristics emerge, providing profound insights into the mechanics and behavior of myofibrils. Calcium spontaneous oscillatory contractions (Ca-SPOC) occurre at partial activation (pCA 6.0-5.5) under isometric condition in myofibrils [17, 20, 34, 37]. During Ca-SPOC, each sarcomere repeat a cycle of slow shortening and rapid lengthening phases in a sawtooth waveform. The consistent oscillatory pattern is sustained for more than 10 seconds without attenuation and can be reproduced well over several repeated cycles of activation and relaxation. The force oscillation waveform gradually changes over time, resulting in an increase in oscillation amplitude and a longer period [17]. Fluctuations could be observed for as long as 1 hour [34].

There is a correlation between length and tension oscillations, where lengthening causes a decrease in tension and shortening an increase in tension [34]. Myofibrils, in which the oscillation once dissipates, do not generate Ca-SPOC after subsequent activations and show steady contraction instead [17]. Addition of 4% PEG, which enhances the intreraction between actin and myosin, suppresses Ca-SPOC activity, allowing measurement of steady force generation at all calcium concentrations [20].

Studying the molecular mechanisms underlying relaxation kinetics is essential to understand the diastolic function of the heart. Experiments demonstrate that the decline in Ca^{2+} occurs before and at a much faster rate than the muscle relaxation [46]. With a fall in Ca^{2+} concentration, Ca^{2+} ions dissociate from troponin. This prevents the formation of new force-generating actomyosin interactions and attached crossbridges dissociate, leading to force decay [47]. While force development can be fitted by a single exponential rate constant k_{act}, force decay is best described by two phases. First, slow initial, almost linear decay with a rate constant k_{lin}, followed by a rapid exponential decay with a rate constant k_{rel} [22].

Passive tension is measured in a relaxing solution with high ATP concentration by stretching myofibrils from their slack length to a specific sarcomere length, and then recording the tension value at the end of the stretch, which is used to plot the sarcomere length-passive tension relationship [19]. Titin is believed to be the source of passive tension in myofibrils [48, 49]. Degradation or extraction of titin from myofibrils lead to a rapid drop in passive force in cardiac myofibrils [50].

Passive force enhancement (PFE) is the difference between the passive forces obtained after passive stretch of the myofibril in relaxing solution and active strech in activation solution [24]. PFE is partly associated with titin as myofibrils show a Ca^{2+} -dependent increase in passive force at long lengths that is independent of actin-myosin crossbridge formation and active force production due to troponin depletion [24, 51]. Moreover, titin is known to increase its stiffness with Ca^{2+}, and at increasing lengths, it becomes more pronounced [52].

Residual force enhancement (RFE) is when a muscle produces a relatively higher force at same final sarcomere length that is reached by stretching while it is actively contracting, as opposed to during a purely isometric contraction where the muscle is held at a fixed length [32]. RFE is known phenomenon of skeletal muscles [26, 53], but when it was initially measured in cardiac papillary and ventricle myofibrils, it was found to be absent [11, 54]. However, recent study has shown that cardiac ventricle myofibrils also exhibit increased forces after active stretching compared with the corresponding purely isometric reference conditions [36].

These glimpses into the inner workings of myofibrils offer a deeper understanding of their machinery and shed light on the fascinating complexities that drive muscle function. Thus, when a corresponding setup for measuring force from single myofibrils is established, it would allow us to study these complex mechanisms in greater detail, providing us with more comprehensive understanding of the inner workings of myofibrils.

2 Materials and methods

2.1 Isolation of myofibrils

All animal procedures were carried out according to the guidelines of Directive 2010/63/EU of the European Parliament on the protection of animals used for scientific purposes and had been approved by the Project Authorisation Committee for Animal Experiments in the Estonian Ministry of Rural Affairs.

The tissue used for isolating myofibrils was dissected from mouse cardiac ventricle muscle. Muscle samples were snap frozen in liquid nitrogen and stored in -80°C or used right after the dissection. The dissected tissue was cut into smaller pieces using a scalpel and weighted. Around 4 to 8 mg of tissue was immersed in 2 ml permeabilization solution, which contained (mM): Tris 10, NaCl 132, KCl 5, $MgCl_2$ 1, EGTA 5, dithiothreitol (DTT) 5, NaN_3 10, BDM 20 and 1% Triton X-100. Protease inhibitors were added and the pH was adjusted to 7.1 with NaOH.

The solution containing the sample was placed on a shaker (BioSan Orbital Shaker PSU-10i) and subjected to agitation (210 RPM) for 3 hours in a cold room at 4 °C. Then, the solution was removed with a pipette and washed in 2 ml washing solution (same as permeabilization solution but without BDM and Triton X-100) for 15 min on shaker.

The solution was changed again and the sample in 2 ml washing solution was transferred to a 10 ml tube, where it was homogenized with a blender (Tissue Tearor model 985370). Homogenization was done at setting 3 (about 15,000 RPM) for 15 seconds. The myofibrils in the homogenate were stored at 4 °C and used for testing the microneedles within a week.

2.2 Fluorescence microscopy

The myofibril suspension with ATP (5 mM) was stained with ATTO 633 phalloidin (ATTO-Tec, Germany) and incubated for 30 minutes to allow binding to the actin filaments within the myofibrils. Imaging was carried out using a laser scanning confocal microscope (Zeiss LSM 900) and with a 63x water immersion objective (NA=1.2). Phalloidin samples were excited using a 640 nm laser.

2.3 Microneedles

Microneedles were prepared from borosilicate glass capillaries (outer diameter 1 mm or 1.5 mm) using a vertical pipette puller (Narishige PC-10) that works by heating and softening the central region of the tube (Figure 4). While the upper end remains stationary, the lower end gradually drops due to the influence of weights. As a result, two tapered capillaries were formed. The weights and heating are adjustable.

Microneedle calibration was done using a force transducer (Aurora Scientific 406A) with sensitivity of 0.05 mN/V and resolution of 10 nN. The force transducer was firmly attached to an inverted microscope (Nikon Eclipse Ti) stage and positioned so that the force sensor

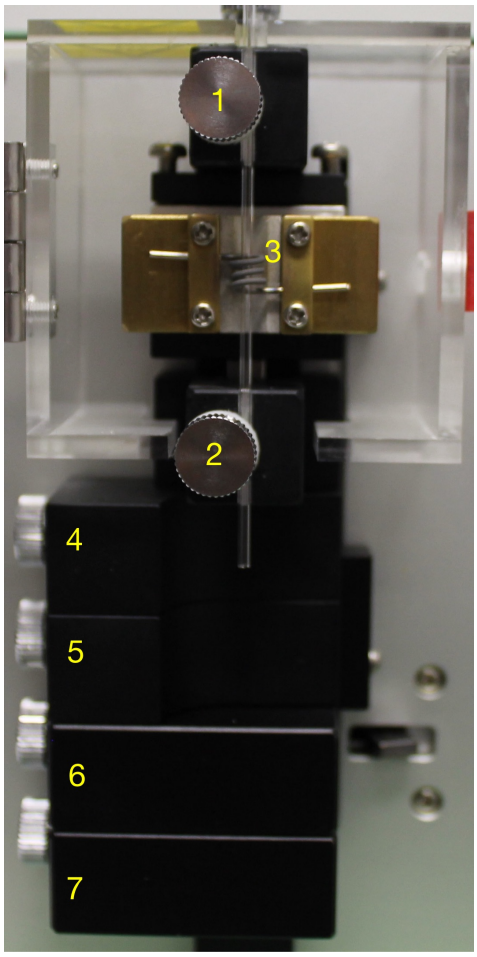

Figure 4. Vertical pipette puller with a mounted glass capillary. The numbers on the figure indicate: 1 - upper end holder; 2 - lower end holder; 3 - heating filament; 4 to 7 - removable weights. Photograph by Triinu Rätsepso.

would be visible through the microscope objective. The microneedle was connected with a micromanipulator and moved slightly in contact with the sensor. A software, previously developed at the laboratory, was used to move the microneedle against the sensor, resulting in a maximum deflection of 100 µm. With the corresponding values from the force transducer at each position, it calculated the stiffness of the needle. Stiffness was measured at different lengths from the tip and also before and after the experiments to evaluate if and how much glue changed the rigidity. The stiffness values from needles without and with 3145 RTV were compared with the paired t-test. The entire process was monitored in real-time on a computer screen.

Microneedles were precoated with 3145 RTV, Dow Croning or with shellac solution. The shellac solution was prepared in an eppendorf tube with 2 ml of 70% ethanol and 120 mg shellac. The tube with the solution was heated at 65 °C for a minute before usage.

2.4 Experiments

The experimental setup, seen in Figure 5, uses an inverted microscope (Nikon Eclipse Ti) with following elements: left and right micromanipulators (Scientifica) with piezo motors,

micromanipulator controller in XYZ plane for moving the microneedles, microneedle holders and a charge-coupled device (CCD ImperX) for imaging.

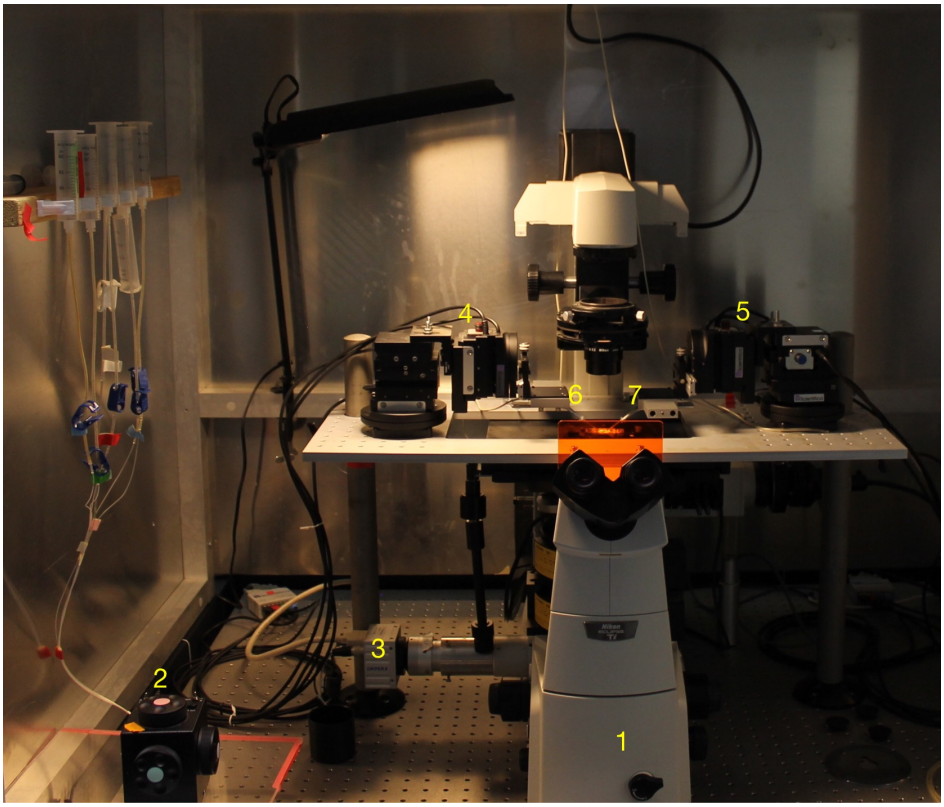

Figure 5. Inverted microscope setup. The numbers on the figure indicate: 1 - inverted microscope; 2 - micromanipulator controller; 3 - CCD; 4 and 5 - left and right piezo motors attached to micromanipulators; 6 and 7 - microneedle holders. Photograph by Triinu Rätsepso.

The experiments were conducted in a perfusion chamber (Figure 6) that was securely positioned on a stage adapter platform. The coverslips of the perfusion chamber were precoated with polyhydroxyethylmethacrylate (poly-HEMA) solution (5% poly-HEMA in 95% ethanol, w/v). The poly-HEMA solution was pipetted (approximately 75 µl) on the slide, spread around with another glass slide and left to dry at least for an hour. Without the coating, the myofibrils sunk to the bottom sticked to the glass slide and would not attach to the needles.

Relaxing solution containing ATP is pipetted into the chamber, followed by an addition of a

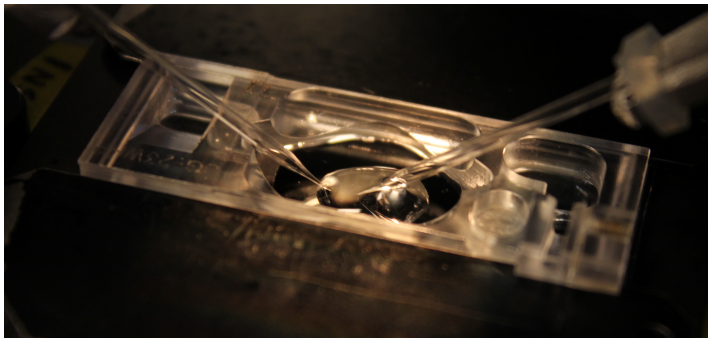

Figure 6. Perfusion chamber with microneedles attached to a myofibril in relaxing solution. Photograph by Triinu Rätsepso.

small droplet of myofibril suspension. The solution ratio is about 10:1 respectively, depending on the yield of myofibrils in the solution. If more myofibrils are present, less myofibril homogenate could be used. The myofibrils were left to settle for 5 to 10 minutes. Using a 4x objective, a suitable myofibril or bundle on the glass surface was selected and positioned in such a way that it would be centered when viewed under the 40x objective.

First, one microneedle was attached perpendicularly to the myofibril by pressing the needle against one end of the myofibril, adding a slight pressure on the coverslide. The procedure was repeated with the other microneedle from the opposite side. The needles were pressing the myofibril on the coverslide for some time (5 to 10 min) till the glue seemed to have cured. Then, the myofibrils were brought a few micrometers above and slightly stretched to see if firm attachment was achieved.

If the myofibrils were long enough, wrapping method was used before the glue cured, securing the attachment even more. When firm attachment was confirmed, calcium was carefully added by a pipette into the chamber and delfection of the needles was observed through CCD on computer monitor. In this study, the microneedles are quite flexible to be able to see the deflection visually by adding pointers on the screen before activation. The distance was measured by moving the deflected needle with the piezo motor to the initial spot, where the pointer was placed.

In case the striation pattern of sarcomeres was visible, sarcomere length was measured using a software previously developed at the laboratory [55] that determines the mean sarcomere length from transmission images.

The experiments took place at room temperature.

3 Results and discussion

3.1 Myofibrils

In the laboratory, the isolation of myofibrils had not been carried out prior to this thesis. Therefore, the method was introduced and optimized until contractive myofibrils were obtained.

The homogenization of muscle tissue did not result in a completely homogeneous solution but rather a heterogeneous one. The suspension mainly contained dispersed distribution of larger and smaller pieces of myofibril bundles. Also, myofibrils have a tendency to clump together and aggregate, resulting in the formation of larger clusters. The yield of myofibrils was best with freshly dissected tissue. The deterioration in quality was observed with myofibrils that were frozen for an extended period. Finding a single myofibril with a visible striation pattern was difficult and often unsuccessful, so mostly bundles of myofibrils were used to assess the flexibility of the microneedles.

The calcium sensitivity of the myofibrils was evaluated in the absence of attached needles by adding calcium into the chamber and monitoring the resulting changes in length. Figure 7 shows, how myofibrils shortened upon the addition of calcium.

Upon exposure to high concentrations of calcium, the presence of remarkably small contracted myofibrils become apparent. During homogenization, the tissue is also fragmented into minuscule pieces that are not visible in the solution. However, when calcium is added, the small myofibrils contract and their density increases, enhancing their visibility under the transmission microscope.

Fluorescence microscopy was used once to visualize the structure of the isolated myofibrils. Staining was done with phalloidin, which binds to the actin filaments (F-actin) in the I-band region, including the Z-lines. To see the myofibril bundle in three dimensions, z-stack acquisition was performed. It involves capturing a series of sections at different focal planes along the z-axis. In Figure 8, a myofibril bundle at various focal levels is seen. The myofibrils

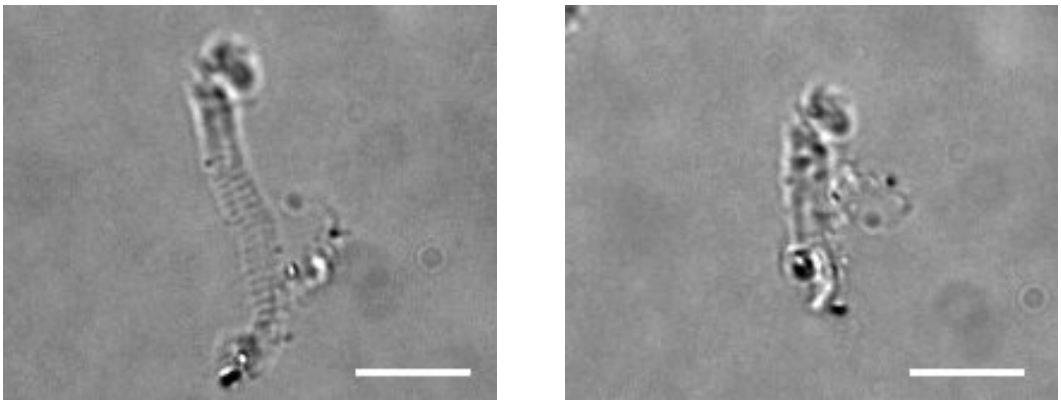

(a) **(b)**

Figure 7. Myofibrils. (a) A bundle of isolated myofibrils in relaxing solution. Subtle striations are noticeable (b) The myofibrils contract in response to an increase in calcium concentration. Scale bars 20 µm.

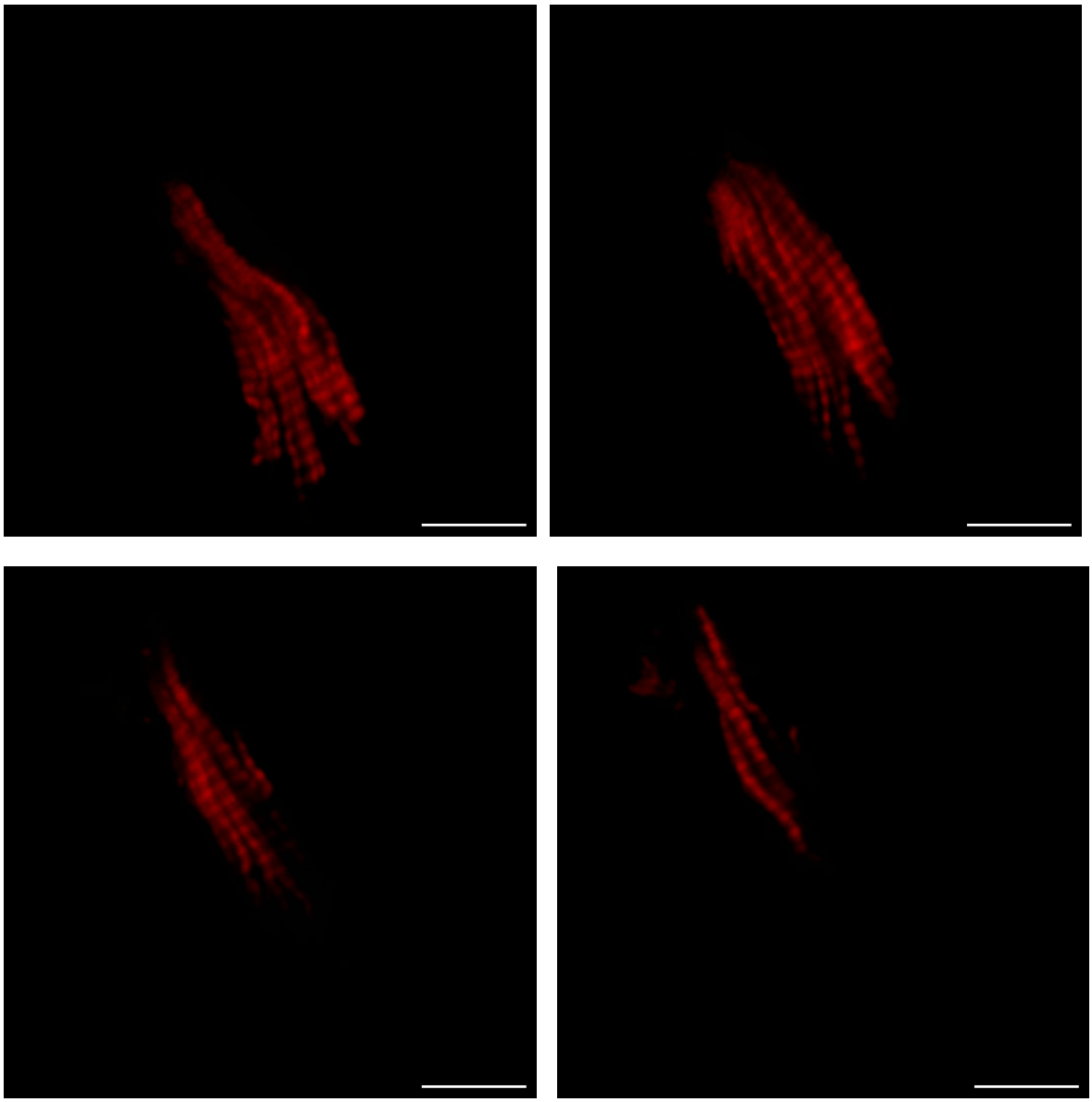

Figure 8. Confocal z-stack images of fluorescence stained myofibrils. Fluorescently stained F-actin with ATTO 633 phalloidin which is located in the I-band. Scale bars 10 µm.

are clearly distinguishable within the bundle and consistent striation pattern is observed. The more intensely stained regions are I-bands and weakly stained areas are A-bands.

3.2 Setup design

The system in this study is designed to measure force from transmission images. In Figure 9, a scheme of the setup is seen. The images are recorded with CCD mounted on the inverted microscope and processed in real-time. The micromanipulators are moved with the controller for positioning and attaching the needles. Piezo motors, which move the microneedles in the range of 100 µm for measuring force, are connected to the micromanipulators and controlled by piezo nanopositioning controller.

The myofibrils, perpendicularly attached to microneedles, are placed at the center of the

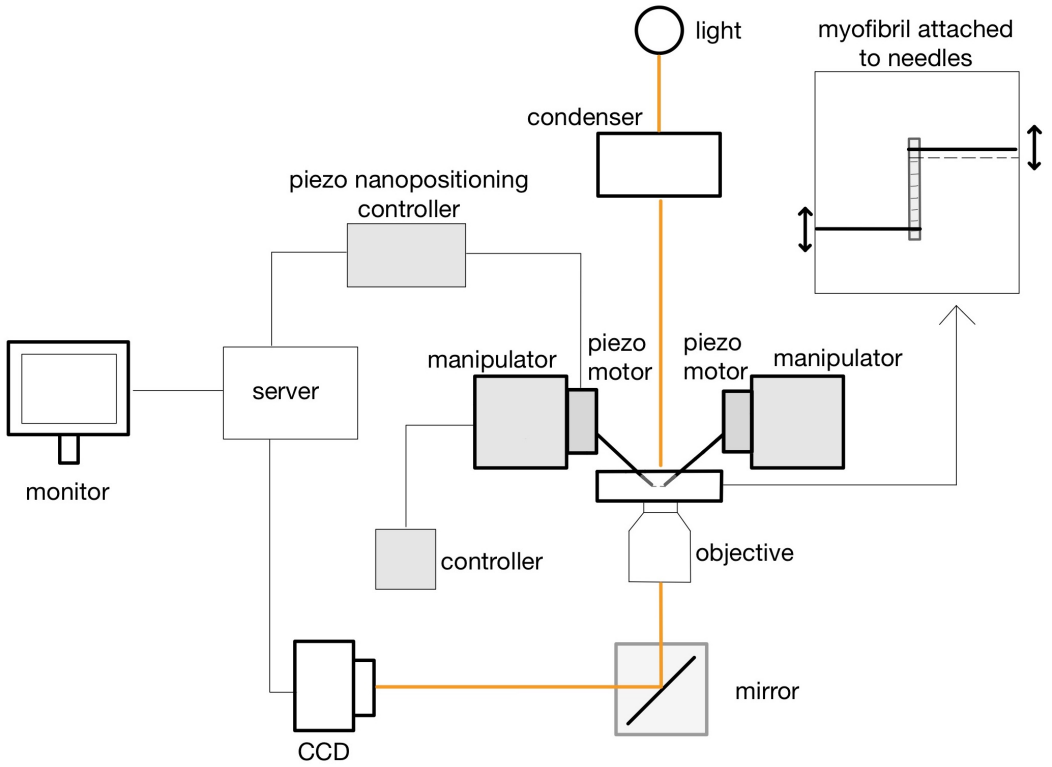

Figure 9. Scheme of the system for force measurements. The light is directed through the condenser onto the sample, and it then passes through the objective lens. From there, the light reflects off a mirror and reaches the CCD. The captured images are processed by real-time Linux server. The insert displays attached microneedles to a myofibril, and the dashed line represents a bent needle. The bending occurs further away from the tip, causing the needle to appear straight in the field of view. The arrows near microneedles indicate piezo motors.

monitor screen and pointers are added on the screen to determine the initial position of the needles. When the the needle moves during contraction, it is repositioned back to the original location where the pointer was added. Currently, the piezo motor's movement for determining the deflected distance is accomplished by incrementing distance values within the software manually. After further testing, the setup will be changed to adjust the position automatically.

The microneedle functions as a cantilever, and when the myofibrils contract, they exert forces that cause the needle to bend. With the deflection distance of the needle and its stiffness, the force can be calculated, if the relation between distance and force follows Hooke's law, where they are linearly dependent on each other. The stiffness of a needle, which in turn affects the magnitude of bending, can be influenced by its characteristics such as length and diameter. While the piezo motor allows for a measurable distance of 100 µm, it is important to ensure that the deflection at maximum force remains within a certain range. This is necessary because the objective is to measure isometric contractions. Additionally, this limitation is due to the typical size range of myofibrils, which spans from 20 to 90 µm. Therefore, it is essential to fabricate microneedles that meet these specific requirements.

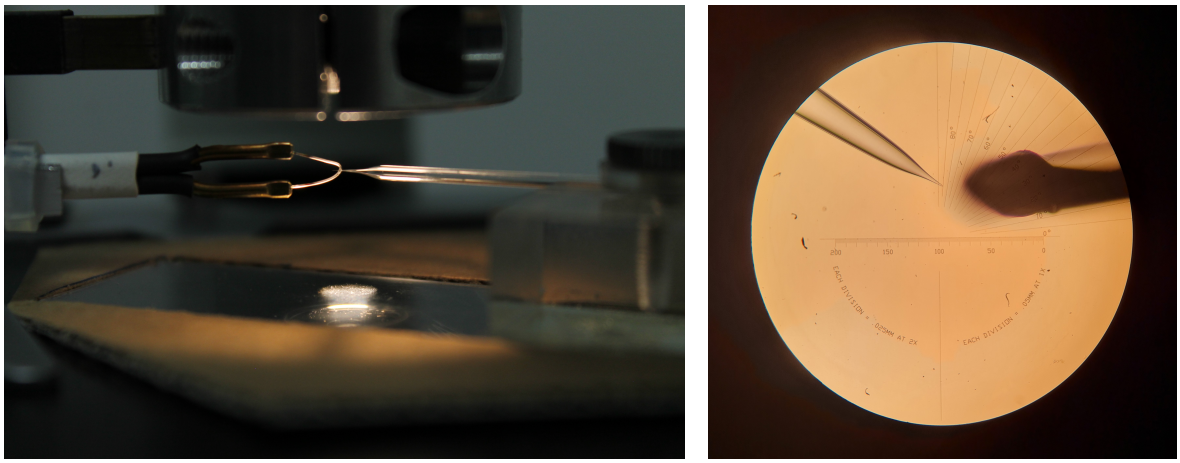

(a) (b)

Figure 10. Microneedle pulling from glass bead. (a) Heating filament (left) and pulled glass capillary (right) under optical microscope. Photograph by Triinu Rätsepso. (b) Image taken through microscope eyepiece of glass capillary (left) positioned near the glass bead on the heating filament (right) for pulling. The capillary is under an angle and pulled horizontally by moving the microscope stage. The eyepiece scale indicates that each division equals to 5 µm with 10x objective.

3.3 Microneedles

Microneedles were first pulled from 1 mm capillaries with the vertical pipette puller. Different settings were tried by adjusting the temperature and weights. But the needles were too rigid to be even calibrated with the force transducer as the force sensor is very delicate and cannot withstand larger forces than 20 mN. So a different method was needed and glass bead was introduced [56].

Firstly, a glass bead was created under optical microscope by melting glass capillary onto the

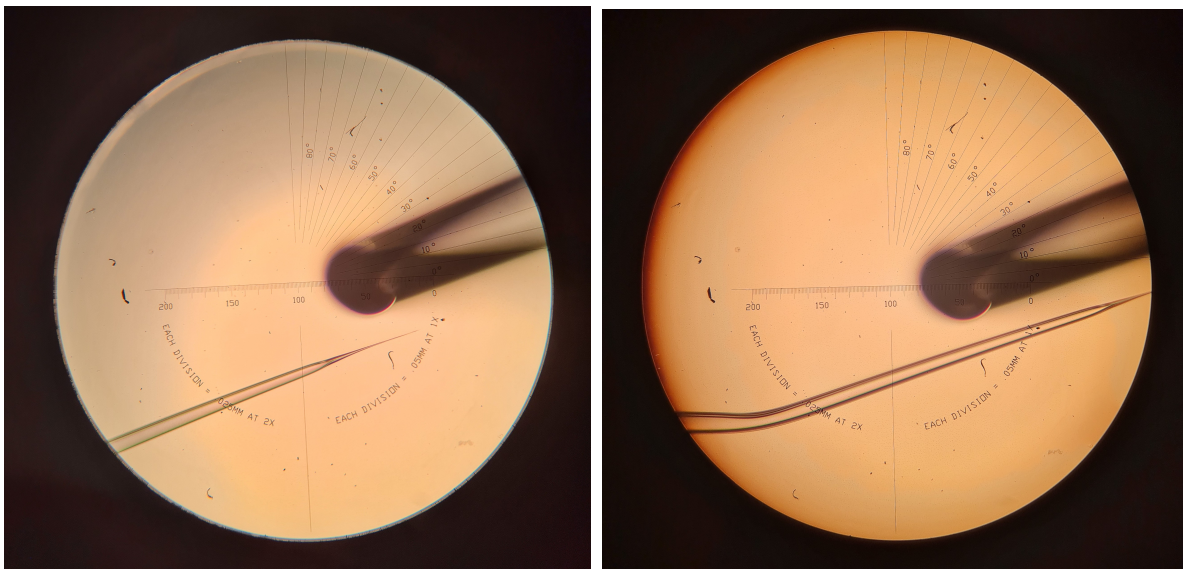

(a) (b)

Figure 11. Glass microneedles. (a) Tip of a two-step drawn microneedle from 1 mm capillary. (b) Bent microneedle after pulling.

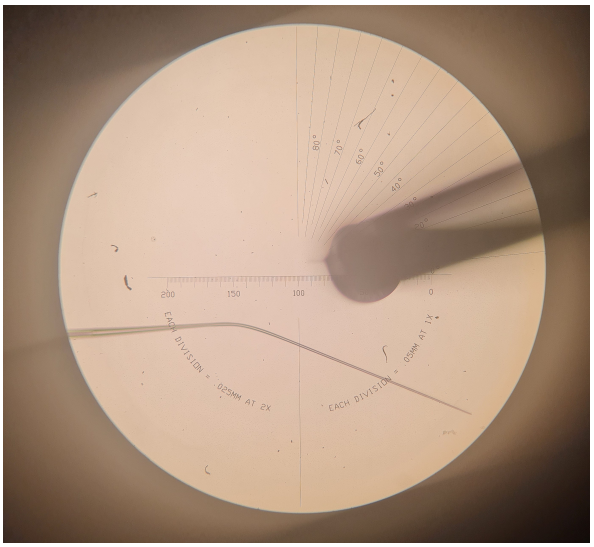

Figure 12. Microneedle tip with a nearly uniform diameter.

microforge heating filament that is attached to the microscope objective. Glass capillaries were held in a pipette holder and moved with the microscope stage. Then, the pulled glass with tapered end was horizontally positioned with the heating filament, allowing its tip to come into contact with the bead. Heat was applied and as soon as the tip and glass bead fused together, the glass rod was pulled away from the bead, stretching the fused part longer. For aligning the cantilever parallel to the specimen, the pipette was bent by heating at about 1 mm from its tip to an angle below 35 °. To facilitate the process, the pulling from the glass bead was done under an angle so that further bending was not required (Figure 10).

This method enabled to pull a thinner cantilever tip, which was more pliable (Figure 11). But the calibration showed that the stiffness was not linear and thus incompatible for force

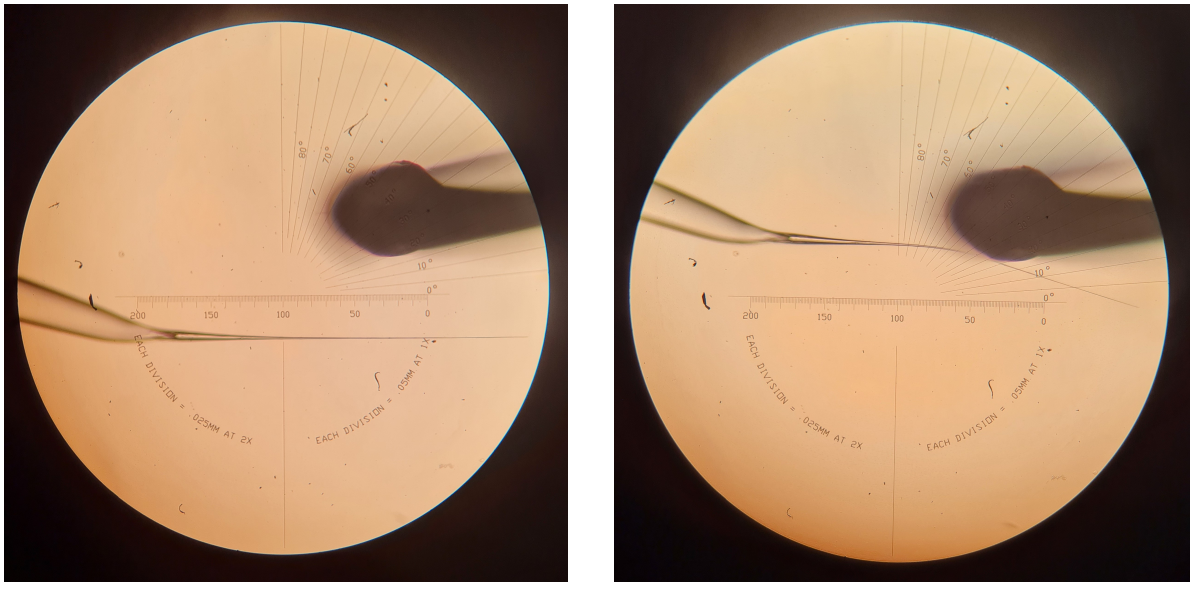

(a) **(b)**

Figure 13. Final design of microneedles. (a) Microneedle cantilever pulled from 1.5 mm capillary. (b) Microneedle pushed against the solid glass bead, showing its flexibility.

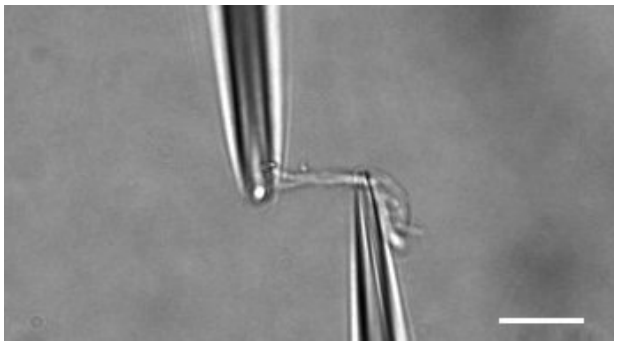

Figure 14. Microneedles attached to myofibrils without glue under 40x objective. Needles pulled only with pipette puller from 1 mm capillaries. Scale bar 20 µm.

measurements. The tip diameter had to be more or less uniform along the cantilever. Pulling the tip to longer lengths from the bead was challanging. The final length depended on the initial taper diameter before pulling from the bead. Thereby, the first pulling had to be optimized accordingly. The sucess rate for pulling a uniform cantilever, seen in Figure.12, from 1 mm capillary was low. Thus, thicker, 1.5 mm glass capillaries were used, which yielded good microneedles for force measurements (Figure 13).

The microneedle stiffnesses varied from 10 to 200 nN/µm. The calibration was done at different locations at the tip, which showed a consistent stiffness. Performing measurements before and after gluing the needles assured that the glue did not change the rigidity of the needle (p-value > 0.19; see Supplementary Table 1) , except when the glue coating diameter was many times larger than the diameter of the microneedle.

3.4 Experiments

The experiments primarily involved testing various needles and attachment methods. At first, the experiments were conducted without gluing the needles. The myofibrils adhere to glass quite well, but the problem arised during the second needle attachment. If one needle was attached, the other typically set loose and firm fixation was not achieved. The overlapping method was not possible due to the myofibirl loosening before the wrapping could be completed. Figure 14 shows myofibrils loosely attached to rigid glass needles.

First glue used was silicone adhesive 3145 RTV. A small quantity of adhesive was put on a glass coverslide and the needle was gently brought into contact with it. Then, the needle was lightly brushed against the glass by sliding it along the plane of the coverslide, without bending the needle. The needle tip was always parallel to the glass slide. This was done to remove the excess glue, otherwise the coating would be too thick, altering the needle stiffness. The hole process does not need to be conducted under a microscope. Although the needle tip is very small, it remains visible to the naked eye. Maintaining control over the pressure applied to the needle during the gluing process, without causing it to break, proved to be challenging at first. But with enough practise, it gradually became manageable.

The coated needle was mounted on the micromanipulator and attached to the myofibril right away. Initially, the adhesive coated needles worked really well, with efficiently attaching

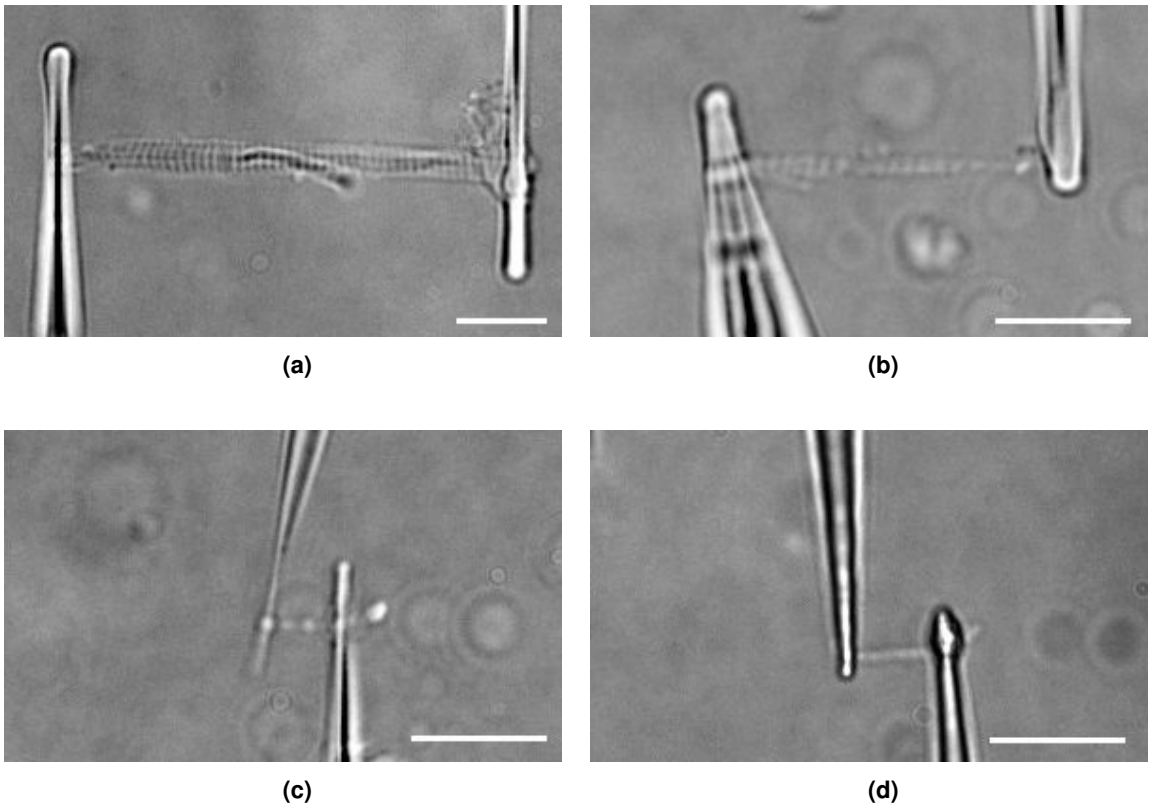

Figure 15. Myofibrils attached to microneedles with glue. The figures show how the isolated myofibrils vary in size with bundles usually being longer. (a) to (c) Needles coated with 3145 RTV. (d) Needles coated with shellack. Scale bars 20 µm.

to myofibrils, but the repetitive opening and closing of the tube made it start to dry and effectiveness declined. So different apporoach was taken by changing the glue and using the shellack solution instead. It also gave quite satisfying results, alleviating concerns about the solution drying out. Another advantage of shellac solution as opposed to silicone adhesive is that it has a much lower viscosity, making it easier to avoid breaking the needle tip while gluing.

Howerver, both adhesives were insufficient in securing the attachment for accurate force measurements. When calcium was introduced to initiate contraction, the myofibrils typically disengaged from the needle, causing minimal or no deflection of the microneedle. When the needles were subjected to tension by stretching the myofibrils prior to calcium addition, it was observed that during contraction the needles showed an outward movement, contrary to the expected inward direction associated with force generation. This confirmed that myofibrils indeed tend to loosen, making it challenging to measure force accurately. Hence, it was necessary to wrap the myofibrils around the glue coated microneedle tips. The wrapping method secured the attachment and a few successful deflections were observed, with the needle bending a couple of micrometers. However, single myofibrils were often not long enough for the wrapping method. In Figure 15, the discernible variations in length between individual and bundles of myofibrils can be seen. Additionally, there was a constant risk of overstretching and damaging the myofibrils during the wrapping process.

3.5 Current limitations and future directions

Although this system overall works, many aspects are in need for improvement. Firstly, the isolation of myofibrils should yield more longer single myofibrils. This would be done by optimizing the homogenization protocol and muscle tissue preservation. Next, it is expected that the image contrast needs to be improved by using phase contrast techniques. For that, we plan to extend the microscope with the corresponding optical elements.

The microneedle detection will be revised. The software, previously used in the laboratory for myocyte kinetics [57] , works on the principle of tracking black objects. Thus, there are two options; whether to tune the software or color the needles darker. Closer to that stage, we would have to analyze light intensity profiles on the current and colored needles and will use the simplest possible method.

The next step is to use a perfusion system with activating and relaxing solution, to initiate repeated contractions and evaluate the force decline. Target is to get several contraction cycles, as is usually specified in the methods of other papers in the field [16, 26], without significant force decline. Then, the myofibrils are eligible for experiments assessing force development at different calcium concentrations.

Conclusion

A system for single myofibril force measurements was put together. This involved designing microneedles that deflect during myofibril contraction. Several types of needles were tested until the optimal microneedles were developed. The myofibril isolation protocol was established and optimized until myofibrils that exhibit calcium sensitivity were successsfully isolated and used for the experiments with the microneedles. The best attachment was achieved by coating the tips of the microneedles with shellac solution and wrapping the myofibrils around the tips. Despite numerous complications, microneedle deflection during calcium induced contraction was eventually observed, making this system a promising apparatus for single myofibril force measurements.

The system will be further developed to enable accurate measurement of force at different calcium concentrations.

Acknowledgments

I would like to express gratitude to my supervisors, Marko Vendelin and Martin Laasmaa for giving me an opportunity to work on such an interesting topic and guiding me along the way, and Rikke Birkedal and Jelena Branovets for their assistance in the biological aspects of this thesis. Also, I would like to thank Triinu Rätsepso for photographing the experimental setup and overall keeping the motivation up.

This work was supported, in part, by the Estonian Research Council (PRG1127).

References

[1] Emmons-Bell, S., Johnson, C. & Roth, G. Prevalence, incidence and survival of heart failure: A systematic review. *Heart* **108**, 1351–1360 (2022).

[2] Savarese, G. & Lund, L. H. Global Public Health Burden of Heart Failure. *Cardiac Failure Review* **3**, 7–11 (2017).

[3] Groenewegen, A., Rutten, F. H., Mosterd, A. & Hoes, A. W. Epidemiology of heart failure. *European Journal of Heart Failure* **22**, 1342–1356 (2020).

[4] Huxley, A. F. & Niedergerke, R. Structural Changes in Muscle During Contraction: Interference Microscopy of Living Muscle Fibres. *Nature* **173**, 971–973 (1954).

[5] Huxley, H. & Hanson, J. Changes in the Cross-Striations of Muscle during Contraction and Stretch and their Structural Interpretation. *Nature* **173**, 973–976 (1954).

[6] Crocini, C. & Gotthardt, M. Cardiac sarcomere mechanics in health and disease. *Biophysical Reviews* **13**, 637–652 (2021).

[7] Ahmed, R. E., Tokuyama, T., Anzai, T., Chanthra, N. & Uosaki, H. Sarcomere maturation: Function acquisition, molecular mechanism, and interplay with other organelles. *Philosophical Transactions of the Royal Society B: Biological Sciences* **377**, 20210325 (2022).

[8] Taylor, K. A., Taylor, D. W. & Schachat, F. Isoforms of α-Actinin from Cardiac, Smooth, and Skeletal Muscle Form Polar Arrays of Actin Filaments. *The Journal of Cell Biology* **149**, 635–646 (2000).

[9] Geeves, M. A., Fedorov, R. & Manstein, D. J. Molecular mechanism of actomyosin-based motility. *Cellular and Molecular Life Sciences CMLS* **62**, 1462–1477 (2005).

[10] Vikhorev, P. G., Ferenczi, M. A. & Marston, S. B. Instrumentation to study myofibril mechanics from static to artificial simulations of cardiac cycle. *MethodsX* **3**, 156–170 (2016).

[11] Shalabi, N., Cornachione, A., de Souza Leite, F., Vengallatore, S. & Rassier, D. E. Residual force enhancement is regulated by titin in skeletal and cardiac myofibrils. *The Journal of Physiology* **595**, 2085–2098 (2017).

[12] Leite, F. S. *et al.* Reduced passive force in skeletal muscles lacking protein arginylation. *American Journal of Physiology - Cell Physiology* **310**, C127–C135 (2016).

[13] Stehle, R., Krüger, M. & Pfitzer, G. Force kinetics and individual sarcomere dynamics in cardiac myofibrils after rapid ca(2+) changes. *Biophysical Journal* **83**, 2152–2161 (2002).

[14] Scellini, B. *et al.* Mavacamten has a differential impact on force generation in myofibrils from rabbit psoas and human cardiac muscle. *The Journal of General Physiology* **153**, e202012789 (2021).

[15] Woulfe, K. C. *et al.* A Novel Method of Isolating Myofibrils From Primary Cardiomyocyte Culture Suitable for Myofibril Mechanical Study. *Frontiers in Cardiovascular Medicine* **6**, 12 (2019).

[16] Pavlov, I., Novinger, R. & Rassier, D. E. The mechanical behavior of individual sarcomeres of myofibrils isolated from rabbit psoas muscle. *American Journal of Physiology. Cell Physiology* **297**, C1211–1219 (2009).

[17] Shimamoto, Y., Suzuki, M. & Ishiwata, S. Length-dependent activation and auto-oscillation in skeletal myofibrils at partial activation by Ca2+. *Biochemical and Biophysical Research Communications* **366**, 233–238 (2008).

[18] Yang, P., Tameyasu, T. & Pollack, G. H. Stepwise dynamics of connecting filaments measured in single myofibrillar sarcomeres. *Biophysical Journal* **74**, 1473–1483 (1998).

[19] Linke, W. A., Popov, V. I. & Pollack, G. H. Passive and active tension in single cardiac myofibrils. *Biophysical Journal* **67**, 782–792 (1994).

[20] Bartoo, M. L., Popov, V. I., Fearn, L. A. & Pollack, G. H. Active tension generation in isolated skeletal myofibrils. *Journal of Muscle Research and Cell Motility* **14**, 498–510 (1993).

[21] van de Locht, M., de Winter, J. M., Rassier, D. E., Helmes, M. H. B. & Ottenheijm, C. A. C. Isolating Myofibrils from Skeletal Muscle Biopsies and Determining Contractile Function with a Nano-Newton Resolution Force Transducer. *Journal of Visualized Experiments: JoVE* (2020).

[22] Stehle, R. *et al.* Isometric force kinetics upon rapid activation and relaxation of mouse, guinea pig and human heart muscle studied on the subcellular myofibrillar level. *Basic Research in Cardiology* **97 Suppl 1**, I127–135 (2002).

[23] ter Keurs, H. E., Rijnsburger, W. H., van Heuningen, R. & Nagelsmit, M. J. Tension development and sarcomere length in rat cardiac trabeculae. Evidence of length-dependent activation. *Circulation Research* **46**, 703–714 (1980).

[24] Joumaa, V., Rassier, D. E., Leonard, T. R. & Herzog, W. Passive force enhancement in single myofibrils. *Pflügers Archiv - European Journal of Physiology* **455**, 367–371 (2007).

[25] Sokolov, S. Yu. *et al.* “Minimum average risk” as a new peak-detection algorithm applied to myofibrillar dynamics. *Computer Methods and Programs in Biomedicine* **72**, 21–26 (2003).

[26] Rassier, D. E. Pre-power stroke cross bridges contribute to force during stretch of skeletal muscle myofibrils. *Proceedings of the Royal Society B: Biological Sciences* **275**, 2577–2586 (2008).

[27] Haeger, R., de Souza Leite, F. & Rassier, D. E. Sarcomere length non-uniformities dictate force production along the descending limb of the force–length relation. *Proceedings of the Royal Society B: Biological Sciences* **287**, 20202133 (2020).

[28] Trecarten, N., Minozzo, F. C., Leite, F. S. & Rassier, D. E. Residual force depression in single sarcomeres is abolished by MgADP-induced activation. *Scientific Reports* **5**, 10555 (2015).

[29] Fauver, M. E., Dunaway, D. L., Lilienfeld, D. H., Craighead, H. G. & Pollack, G. H. Microfabricated cantilevers for measurement of subcellular and molecular forces. *IEEE transactions on bio-medical engineering* **45**, 891–898 (1998).

[30] Shalabi, N., Persson, M., Månsson, A., Vengallatore, S. & Rassier, D. E. Sarcomere Stiffness during Stretching and Shortening of Rigor Skeletal Myofibrils. *Biophysical Journal* **113**, 2768–2776 (2017).

[31] Tesi, C., Piroddi, N., Colomo, F. & Poggesi, C. Relaxation kinetics following sudden Ca(2+) reduction in single myofibrils from skeletal muscle. *Biophysical Journal* **83**, 2142–2151 (2002).

[32] Haeger, R. M. & Rassier, D. E. Force enhancement after stretch of isolated myofibrils is increased by sarcomere length non-uniformities. *Scientific Reports* **10**, 21590 (2020).

[33] Shimamoto, Y., Kono, F., Suzuki, M. & Ishiwata, S. Nonlinear force-length relationship in the ADP-induced contraction of skeletal myofibrils. *Biophysical Journal* **93**, 4330–4341 (2007).

[34] Linke, W. A., Bartoo, M. L. & Pollack, G. H. Spontaneous sarcomeric oscillations at intermediate activation levels in single isolated cardiac myofibrils. *Circulation Research* **73**, 724–734 (1993).

[35] Iwazumi, T. High-speed ultrasensitive instrumentation for myofibril mechanics measurements. *The American Journal of Physiology* **252**, C253–262 (1987).

[36] Han, S.-w., Boldt, K., Joumaa, V. & Herzog, W. Characterizing residual and passive force enhancements in cardiac myofibrils. *Biophysical Journal* (2023).

[37] Kagemoto, T. *et al.* Sarcomeric Auto-Oscillations in Single Myofibrils From the Heart of Patients With Dilated Cardiomyopathy. *Circulation: Heart Failure* **11**, e004333 (2018).

[38] Anazawa, T., Yasuda, K. & Ishiwata, S. Spontaneous oscillation of tension and sarcomere length in skeletal myofibrils. Microscopic measurement and analysis. *Biophysical Journal* **61**, 1099–1108 (1992).

[39] Labuda, A., Brastaviceanu, T., Pavlov, I., Paul, W. & Rassier, D. E. Optical detection system for probing cantilever deflections parallel to a sample surface. *The Review of Scientific Instruments* **82**, 013701 (2011).

[40] Harrison, S. M., Lamont, C. & Miller, D. J. Hysteresis and the length dependence of calcium sensitivity in chemically skinned rat cardiac muscle. *The Journal of Physiology* **401**, 115–143 (1988).

[41] Belus, A. *et al.* The familial hypertrophic cardiomyopathy-associated myosin mutation R403Q accelerates tension generation and relaxation of human cardiac myofibrils. *The Journal of Physiology* **586**, 3639–3644 (2008).

[42] Ma, Y. Z. & Taylor, E. W. Kinetic mechanism of myofibril ATPase. *Biophysical Journal* **66**, 1542–1553 (1994).

[43] Stehle, R., Lionne, C., Travers, F. & Barman, T. Kinetics of the initial steps of rabbit psoas myofibrillar ATPases studied by tryptophan and pyrene fluorescence stopped-flow and rapid flow-quench. Evidence that cross-bridge detachment is slower than ATP binding. *Biochemistry* **39**, 7508–7520 (2000).

[44] Kobirumaki-Shimozawa, F. *et al.* Cardiac thin filament regulation and the Frank–Starling mechanism. *The Journal of Physiological Sciences* **64**, 221–232 (2014).

[45] Green, E. M. *et al.* A small-molecule inhibitor of sarcomere contractility suppresses hypertrophic cardiomyopathy in mice. *Science* **351**, 617–621 (2016).

[46] Brutsaert, D. L. & Sys, S. U. Relaxation and diastole of the heart. *Physiological Reviews* **69**, 1228–1315 (1989).

[47] Poggesi, C., Tesi, C. & Stehle, R. Sarcomeric determinants of striated muscle relaxation kinetics. *Pflugers Archiv: European Journal of Physiology* **449**, 505–517 (2005).

[48] Linke, W. A. *et al.* Towards a molecular understanding of the elasticity of titin. *Journal of Molecular Biology* **261**, 62–71 (1996).

[49] Cazorla, O. *et al.* Differential expression of cardiac titin isoforms and modulation of cellular stiffness. *Circulation Research* **86**, 59–67 (2000).

[50] Opitz, C. A. *et al.* Damped elastic recoil of the titin spring in myofibrils of human myocardium. *Proceedings of the National Academy of Sciences of the United States of America* **100**, 12688–12693 (2003).

[51] Joumaa, V., Rassier, D. E., Leonard, T. R. & Herzog, W. The origin of passive force enhancement in skeletal muscle. *American Journal of Physiology-Cell Physiology* **294**, C74–C78 (2008).

[52] Labeit, D. *et al.* Calcium-dependent molecular spring elements in the giant protein titin. *Proceedings of the National Academy of Sciences of the United States of America* **100**, 13716–13721 (2003).

[53] Joumaa, V., Leonard, T. & Herzog, W. Residual force enhancement in myofibrils and sarcomeres. *Proceedings of the Royal Society B: Biological Sciences* **275**, 1411–1419 (2008).

[54] Cornachione, A. S., Leite, F., Bagni, M. A. & Rassier, D. E. The increase in non-cross-bridge forces after stretch of activated striated muscle is related to titin isoforms. *American Journal of Physiology - Cell Physiology* **310**, C19–C26 (2016).

[55] Peterson, P., Kalda, M. & Vendelin, M. Real-time determination of sarcomere length of a single cardiomyocyte during contraction. *American Journal of Physiology. Cell Physiology* **304**, C519–531 (2013).

[56] Shimamoto, Y. & Kapoor, T. M. Microneedle-based analysis of the micromechanics of the metaphase spindle assembled in Xenopus laevis egg extracts. *Nature protocols* **7**, 959–969 (2012).

[57] Kalda, M. *Mechanoenergetics of a Single Cardiomyocyte*. Ph.D. thesis, Tallinn University of Technology, Tallinn (2015).

Supplementary

Supplementary 1 Microneedle stiffnesses

Table 1. Microneedle stiffnesses without and with 3145 RTV

without glue [N/m]	with glue [N/m]
0.062	0.057
0.02	0.02
0.03	0.024
0.007	0.006
0.025	0.026
0.122	0.17
0.067	0.069
0.005	0.005
0.013	0.015
0.01	0.012
0.027	0.03
0.018	0.019
0.033	0.034
0.014	0.013
0.04	0.04
0.034	0.036
0.134	0.137
0.121	0.139
0.198	0.201
0.065	0.061